

Diffusion of an adsorbed particle: Dependence on the adatom-substrate interaction

Göran Wahnström

Institute of Theoretical Physics, Chalmers University of Technology, S-412 96 Göteborg, Sweden

(Received 8 July 1985)

Based on a general microscopic theory given in an earlier paper we present here a study of the diffusive motion of an atom adsorbed on a solid surface. This is done through an investigation of the quasielastic peak in the dynamic structure factor. Its width goes to zero at each reciprocal-lattice point and the q dependence is found to contain valuable information on the mechanism for the diffusion process. The theory incorporates the dynamics of the adatom-substrate interaction in a more proper way than by using the Brownian-motion theory. All calculations are performed at a temperature corresponding to thermally activated diffusion. If the adatom is identical to the substrate atoms the diffusion process is well described by a jump diffusion model. For a more weakly bound adatom the situation is more complicated. Because of the small friction in this case, adatoms escape only slowly whenever their initial energy is less than the barrier energy for diffusion. On the other hand, adatoms with higher energies move rather freely and give rise to a large contribution to the diffusion constant.

I. INTRODUCTION

In a recent paper,¹ hereafter referred to as I, a microscopic theory for the motion of a single atom adsorbed on a solid surface was proposed. All the important dynamics of the substrate excitations were contained in a certain memory function. Appropriate approximations of this function was presented, based on mode-coupling ideas, familiar from other fields of physics.² Up to now we have only considered the coupling to the phonon modes, but there is no difficulty in including other excitations such as electron-hole pairs. It was also demonstrated in I that an analysis, based on our mode-coupling approximation (MCA) and applied to a realistic system, can be carried out with a reasonable amount of numerical work.

Our approach is free from the restrictive assumptions behind the ordinary Fokker-Planck equation. By making some further approximations the latter equation was derived together with a microscopic expression for the friction coefficient. This approximation is denoted by FPA. In another paper,³ referred to as II, we showed that the Fokker-Planck equation is seriously in error for light adatoms. However, it was found that if the Debye frequency for the substrate phonons is at least twice as large as the characteristic vibrational frequency for the adatom, the Fokker-Planck equation gives quite accurate results, provided one uses a proper position-dependent friction coefficient (FPA).

Here we shall be mainly concerned with the diffusive motion of the adsorbed atom. This is conveniently studied through the quasielastic peak in the dynamic structure factor $S^s(q\omega)$. Its width is found to contain valuable information on the mechanism for the diffusion process. Ignoring the details of the motion inside each surface lattice cell, we can study how the atom migrates from its initial cell to the surrounding ones as time proceeds. We shall then compare our results with what is obtained from a phenomenological jump diffusion model.

The purpose of this paper is twofold. Firstly, we want to elucidate the mechanism for the diffusion process and we shall do that by investigating the quasielastic peak in $S^s(q\omega)$. Secondly, by using our microscopic theory we will show that in some cases a simple jump diffusion model describes the diffusive motion quite well. In other cases this is not true, and an uncritical application of such a model would lead to an incorrect interpretation of the physics involved.

The paper is organized as follows: In the next section we recapitulate the most relevant parts of the theory. A generalized dynamic structure factor and an expression for the time dependence of the probability of finding the adatom in different cells are introduced in Sec. III. The jump diffusion model is presented in Sec. IV and it is followed in Sec. V by a presentation of our numerical results. These are discussed in Sec. VI and we end by making some general remarks and by summarizing the main conclusions in Sec. VII.

II. BASIC FORMULATION

For the sake of completeness we briefly outline the theory in this section. We follow the notation in I and for further details we refer to the previous paper.

The starting point is the following formally exact transport equation [cf. Eq. (4) of I; equations of the previous paper will be abbreviated as (I.4), e.g.]

$$\left[\frac{\partial}{\partial t} + \frac{\mathbf{p}_1}{m} \cdot \nabla_{\mathbf{r}_1} + \mathbf{F}^{\text{ad}}(\mathbf{r}_1) \cdot \nabla_{\mathbf{p}_1} \right] C^s(11't) = \int_0^t d\bar{t} \int d\bar{1} \nabla_{\mathbf{p}_1} \cdot \underline{L}(1\bar{1}t - \bar{t}) \cdot \left[\frac{\beta}{m} \bar{\mathbf{p}}_1 + \nabla_{\bar{\mathbf{p}}_1} \right] C^s(\bar{1}\bar{1}'\bar{t}), \quad (1)$$

where $C^s(11't)$ is the correlation function for the microscopic phase-space density of the adparticle. 1 is a short-

hand notation for the phase-space point $(\mathbf{r}_1, \mathbf{p}_1)$ and $\beta = 1/k_B T$ is the inverse temperature. The influence from the surrounding on the adparticle is split into two parts, one static and one dynamic. The static part gives rise to a temperature-dependent conservative force, $\mathbf{F}^{\text{ad}}(\mathbf{r}) = -\nabla V^{\text{ad}}(\mathbf{r})$, and the dynamic part, the memory function $\underline{L}(11't)$, embodies fluctuation and dissipation of energy.

The formulation is general but in the calculations, presented in I, the motion of the adatom was restricted to one dimension (x -direction) with the full three-dimensional motion of the substrate particles retained. This restriction will also be used here but we do not believe that the conclusions we draw from our numerical results in any essential way depend on this restriction. Equation (1) is transformed into a corresponding matrix equation [see (I.27)] by Fourier and Laplace transforming the space and time variables, respectively, and by expanding the momentum dependence in terms of Hermite polynomials. By finally inverting this matrix equation C^s is obtained. From C^s several quantities of particular interest can be extracted and we are here going to concentrate on the dynamic structure factor $S^s(q\omega)$.

The outcome of some different physically plausible approximations for the memory function has been investigated in I and II. The following notation was used:

$$\Gamma_{\mu\nu}(xx't) = \frac{\beta}{m} (\mu\nu)^{1/2} \int dp dp' H_{\mu-1}(p) L^{xx}(xpx'p't) \times H_{\nu-1}(p') \Phi_M(p'), \quad (2)$$

where $H_\mu(p)$ are the Hermite polynomials and $\Phi_M(p)$ is the Maxwell distribution function. In the most general approximation, the mode coupling approximation (MCA), the adatom is coupled nonlinearly to the density fluctuations in the substrate and these are expressed in terms of phonon modes. This approximation incorporates the appropriate time scale for the fluctuating force as well as the dependence of this force on the position of the adatom. It leads us to the evaluation of the following expression:

$$M^{\text{MCA}}(xx't) = \frac{\beta}{m} C_{00}^s(xx't) P(xx't), \quad (3)$$

where M is the Γ_{11} element of the memory function in (2). The motion of the adatom enters through its density correlation function

$$C_{00}^s(xx't) = \langle n(x') \rangle^{-1} \langle n(xt) n(x') \rangle,$$

and the coupling to the substrate atoms and their motion are included in the function $P(xx't)$ [see (I.18)]. For numerical convenience we have approximated higher order elements $\Gamma_{\mu\nu}$ ($\mu, \nu > 1$) according to (I.21), which correctly reproduces their initial values.

If the fluctuations in the substrate are fast compared to the characteristic frequencies of the adatom, $C_{00}^s(xx't)$ in (3) can be replaced by its initial value, $\delta(x-x')$. This simplification leads to the Fokker-Planck approximation (FPA) under the condition that one considers times longer than the typical relaxation time in $P(xx't)$. The position-dependent friction coefficient is then given by the time integral of M .

III. EXPERIMENTAL QUANTITIES

The lattice breaks the translation invariance, and the spatial Fourier transforms of the correlation functions therefore contain two wave vectors, differing by a reciprocal-lattice vector. We introduce the following notation for the intermediate scattering function:

$$F_{nn'}^s(\kappa t) = \langle e^{-iqR^a(t)} e^{iq'R^a(0)} \rangle, \quad (4)$$

where $q = \kappa + (2\pi/a)n$ and $q' = \kappa + (2\pi/a)n'$ with κ restricted to the first Brillouin zone and n, n' being integers. The period of the lattice is denoted by a . The corresponding dynamic structure factor is given by

$$S_{nn'}^s(\kappa\omega) = \frac{1}{2\pi} \sum_{\bar{n}} \langle n \rangle_{\bar{n}} C_{00;nn'}^s(\kappa\omega), \quad (5)$$

where $\langle n \rangle_{\bar{n}}$ are the Fourier components of the mean density (see I.17) and $C_{00;nn'}^s(\kappa\omega)$ is defined in I. $S_{nn'}^s(\kappa\omega)$ fulfills the following sum rule:

$$\int_{-\infty}^{\infty} d\omega S_{nn'}^s(\kappa\omega) = \langle n \rangle_{n-n'}, \quad (6)$$

and the diagonal part is equal to the conventional dynamic structure factor, $S^s(q\omega) \equiv S_{nn}^s(\kappa\omega)$.

For a strictly periodic system and $\kappa=0$, $F_{nn'}^s(\kappa t)$ approaches a finite value as $t \rightarrow \infty$ according to

$$F_{nn'}^s(\kappa=0, t \rightarrow \infty) = \langle n \rangle_n \langle n \rangle_{n'}. \quad (7)$$

This time-independent part shows up as an elastic peak in the frequency spectrum.

Ignoring the motion inside each surface lattice cell, we can study how the adatom migrates from its initial cell to the surrounding ones as time proceeds. The probability of finding the adatom in different cells, $P_j(t)$, can be extracted from F^s . Assuming the initial condition $P_j(t=0) = \delta_{j,0}$, we have

$$P_j(t) = \frac{a}{2\pi} \int_{-\pi/a}^{\pi/a} d\kappa \sum_{n,n'} F_{nn'}^s(\kappa t) D_{nn'}^j(\kappa) \quad (8)$$

with

$$D_{nn'}^j(\kappa) = \frac{\cos(a\kappa j) \sin^2(a\kappa/2)}{(a\kappa/2 + \pi n)(a\kappa/2 + \pi n')}. \quad (9)$$

This function is measured in the field ion microscopic experiments.⁴

IV. JUMP DIFFUSION MODEL

We are going to compare our results with a jump diffusion model. It is commonly assumed that a single jump occurs only to nearest-neighbor sites and that successive jumps are independent of each other. For high temperatures or for a weak adatom-substrate atom interaction the possibility of longer and correlated jumps cannot be discounted. Considering a model which allows jumps to both nearest sites at a rate α_1 and to second-nearest sites at a rate α_2 , the probability distribution $P_j(t)$ is given by⁵

$$P_j(t) = \exp[-(\alpha_1 + \alpha_2)t] \sum_{k=-\infty}^{\infty} I_{j-2k}(\alpha_1 t) I_k(\alpha_2 t), \quad (10)$$

where I_k is the modified Bessel function of order k .

The frequency spectrum becomes purely relaxational due to the neglect of oscillations around the equilibrium positions, and the dynamic structure factor has a simple Lorentzian shape with the half-width at half maximum being equal to

$$\omega_{1/2}(q) = \alpha_1[1 - \cos(qa)] + \alpha_2[1 - \cos(2qa)]. \quad (11)$$

It is periodic in q and for $q \rightarrow 0$ we have $\omega_{1/2}(q) = \frac{1}{2}a^2(\alpha_1 + 4\alpha_2)q^2$. By assuming $\alpha_2 = 0$ the ordinary results for single uncorrelated jumps are obtained. We notice that the contribution to the diffusion constant scales as the square of the jump distance and it implies that even a small jump rate α_2 gives a comparatively large contribution to the diffusion constant.

By using the absolute rate theory (ART)⁶ the escape rate from the initial cell, $\alpha = \alpha_1 + \alpha_2$, can be determined from purely equilibrium quantities, and it is given by

$$\alpha^{\text{ART}} = \left[\frac{2}{\pi m \beta} \right]^{1/2} \frac{1}{Z} e^{-\beta V^{\text{ad}}(0)} \quad (12)$$

with

$$Z = \int_0^a dx e^{-\beta V^{\text{ad}}(x)}. \quad (13)$$

For a deep potential well this formula can be simplified and the prefactor becomes proportional to the vibrational frequency for the adatom.⁷ Formula (12) is believed to give a good estimate of the true rate as long as the interaction is not too weak or too strong.⁸

V. NUMERICAL RESULTS

We now turn to the presentation of the results from our numerical calculations. These will be presented in reduced units, which are denoted by an asterisk superscript and expressed in terms of ϵ , σ , and m . ϵ and σ are the parameters entering the Lennard-Jones potential (14) and m is the mass of the particles.

The system we have been considering is exactly the same as in I. The adsorbed atom moves on a fcc (001) surface and is restricted to follow a specific trajectory corresponding to a minimum energy path. The calculations are done at the same temperature as in I, $T^* = 0.30$, and the only difference lies in varying the strength of the coupling between the adatom and the substrate atoms. The interaction between each pair of substrate atoms is assumed to be the Lennard-Jones 6-12 potential

$$v^{ss}(r) = 4\epsilon \left[\left(\frac{\sigma}{r} \right)^{12} - \left(\frac{\sigma}{r} \right)^6 \right]. \quad (14)$$

For the corresponding interaction between the adatom and a substrate atom we have used the same form and considered two cases: $v^{as} = v^{ss}$ and $v^{as} = \frac{1}{2}v^{ss}$.

The change of the interaction strength affects both the vibrational frequency for the adatom and the potential barrier along the diffusion path. The vibrational frequency, determined from the curvature at the bottom of the potential well, is reduced by a factor of $\sqrt{2}$ and the potential barrier by a factor of 2, when v^{as} is decreased. The friction coefficient for the adatom depends quadratically

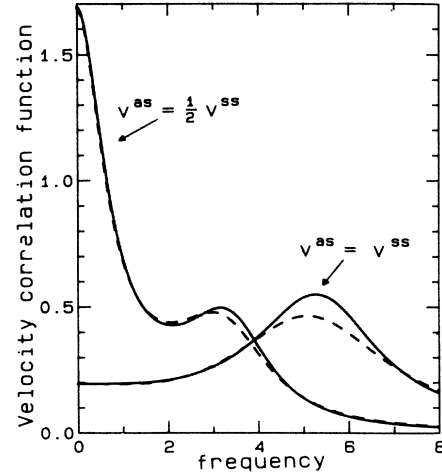


FIG. 1. The frequency spectrum of the velocity correlation function $\phi(\omega)$ for the adatom in reduced units, defined at the beginning of Sec. V. A comparison between MCA (solid curves) and FPA (dashed curves) is shown for two different cases of the adatom-substrate atom interaction potential v^{as} .

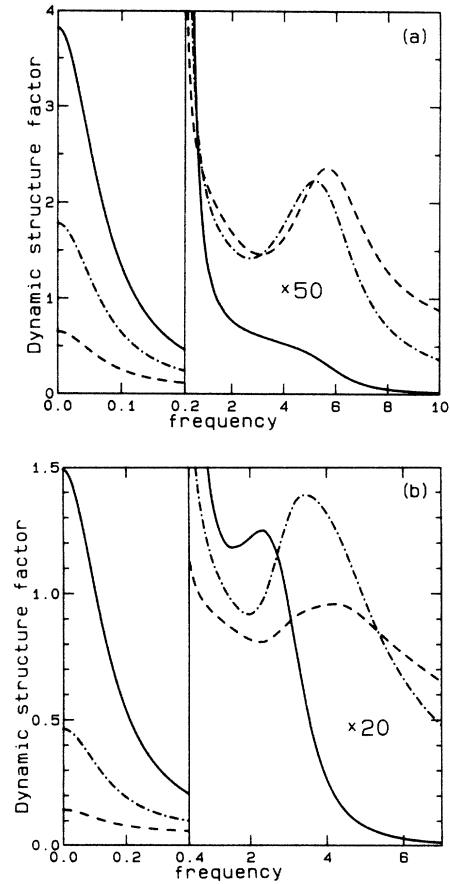


FIG. 2. The dynamic structure factor $S^s(q, \omega)$ as function of frequency in reduced units. Three different q values are shown: $q = \pi/a$ (solid curves), $q = 3\pi/a$ (dotted-dashed curves), and $q = 5\pi/a$ (dashed curves), for two different cases (a) $v^{as} = v^{ss}$ and (b) $v^{as} = \frac{1}{2}v^{ss}$. Notice that the inelastic part is magnified and given in a different frequency scale.

on v^{as} [see (I.11)] and is therefore reduced by a factor of 4. The change of the potential barrier as well as the decrease of the friction is found to have a significant effect on the character of the diffusive motion.

In Fig. 1 we show the change of the frequency spectrum of the velocity correlation function $\phi(\omega)$ for the adatom when v^{as} is reduced. We notice that the vibrational frequency is shifted to lower frequencies, but above all a large quasielastic diffusive peak appears. The diffusion constant D is proportional to $\phi(\omega=0)$ [see (I.30)] and it increases from $D^*=0.029$ to $D^*=0.25$. A comparison between MCA (solid curves) and FPA (dashed curves) is shown in the same figure. One especially notes that the diffusive motion is very well described by FPA. The reason for this is that in both cases the adatom moves on a slower time scale than the substrate atoms. In the following the full MCA will be used but very similar results would be obtained with FPA.

The dynamic structure factor $S^s(q\omega)$ as a function of frequency is shown in Figs. 2(a) ($v^{as}=v^{ss}$) and 2(b) ($v^{as}=\frac{1}{2}v^{ss}$) for three different q values. $S^s(q\omega)$ consists of a quasielastic diffusive peak and for larger wave vectors also an inelastic peak appears. The latter one is caused by the damped oscillations of the adatom within

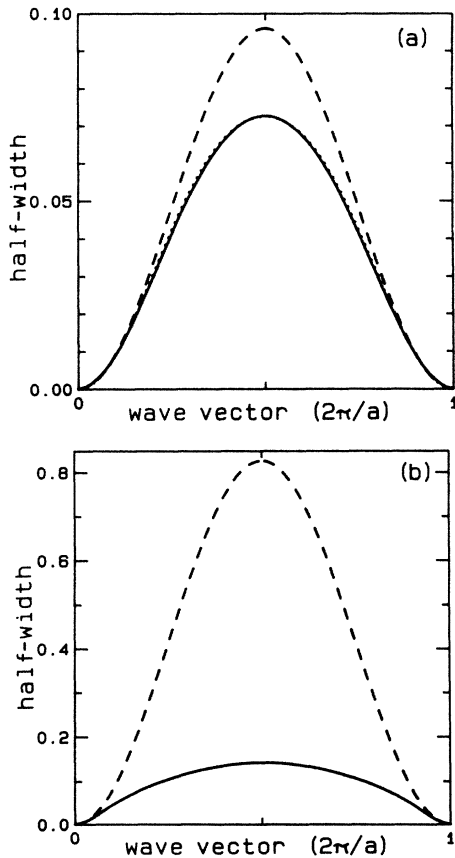


FIG. 3. The half-width at half maximum $\omega_{1/2}(q)$ of the quasielastic peak in $S^s(q\omega)$ in reduced units as function of the wave vector in units of $2\pi/a$. Two different cases are shown: (a) $v^{as}=v^{ss}$ and (b) $v^{as}=\frac{1}{2}v^{ss}$. The MCA results (solid curves) are compared with the jump diffusion model (11) with $\alpha_2/\alpha_1=0.00$ (dashed curves) and $\alpha_2/\alpha_1=0.08$ (dotted curve).

the initial cell and it is most pronounced for intermediate values of the wave vector. The diffusive peak sharpens at every reciprocal-lattice vector to a δ function, and the strength of this function decreases according to formula (7). The inelastic contribution is found to increase in such a way that the sum rule (6) is fulfilled.

In Figs. 3(a) ($v^{as}=v^{ss}$) and 3(b) ($v^{as}=\frac{1}{2}v^{ss}$) we show the half-width at half maximum of the quasielastic peak as a function of q . The width is found to be approximately periodic in q with period $2\pi/a$ but in Fig. 3 we only show the first period. In determining the width we have subtracted the inelastic part. The curvature for small q values gives the diffusion constant, $\omega_{1/2}(q \rightarrow 0) = Dq^2$, and larger q values turn out to give information on the diffusion process itself. The strength of the elastic peak at the reciprocal-lattice points determines the Fourier components of the mean density, according to (7). We have obtained the following values for $\langle n \rangle_n$. In the case

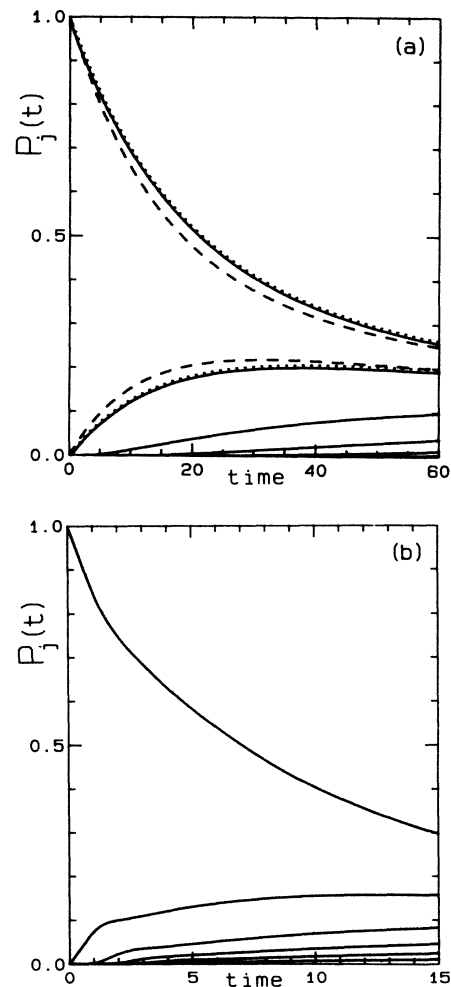


FIG. 4. The time dependence of the probability $P_j(t)$, to find the adatom in the cells $j=0, 1, 2, 3, 4$, and 5 with $P_j(t=0)=\delta_{j,0}$. The time is given in reduced units and two different cases are shown: (a) $v^{as}=v^{ss}$ and (b) $v^{as}=\frac{1}{2}v^{ss}$. In (a) the MCA results (solid curves) are compared with the jump diffusion model (10) with $\alpha_2/\alpha_1=0.00$ (dashed curves) and $\alpha_2/\alpha_1=0.08$ (dotted curves).

$v^{as}=v^{ss}$ we have 1.00, -0.74, 0.45, and -0.25 for $n=0, 1, 2$, and 3, respectively, and in the other case, $v^{as}=\frac{1}{2}v^{ss}$, the corresponding values are 1.00, -0.44, 0.19, and -0.08. This implies that the quasielastic diffusive peak becomes weaker for larger q values and it is possible to extract the width if $q \lesssim 6\pi/a$ for $v^{as}=v^{ss}$ and if $q \lesssim 4\pi/a$ for $v^{as}=\frac{1}{2}v^{ss}$.

In order to reveal the character of the diffusion process we have calculated the time dependence of the probability of finding the adatom in different cells, $P_j(t)$, from Eq. (8). This is shown in Fig. 4(a) ($v^{as}=v^{ss}$) and 4(b) ($v^{as}=\frac{1}{2}v^{ss}$).

Our results are compared in Figs. 3(a), 3(b), and 4(a) with those obtained from the jump diffusion model, (10) and (11), using the calculated MCA value for the macroscopic diffusion constant in all cases.

VI. DISCUSSION

Two different kinds of effects influence the value of the diffusion constant: the escape rate from the initial lattice cell and the jump distance. The escape rate can be estimated using formula (12) and if we assume single uncorrelated jumps with distance a , we get $D_{ART}^*=0.024$ for $v^{as}=v^{ss}$ and $D_{ART}^*=0.094$ for $v^{as}=\frac{1}{2}v^{ss}$. This should be compared with the values $D^*=0.029$ and $D^*=0.25$, respectively, obtained from MCA.

A. $v^{as}=v^{ss}$

In Figs. 3(a) and 4(a) we have compared our results with those obtained from single uncorrelated jumps ($\alpha_2/\alpha_1=0.00$) and from the model containing a small probability of second-neighbor jumps ($\alpha_2/\alpha_1=0.08$). By inspection of these figures we conclude that a simple jump model describes the diffusive motion quite well. This is particularly true if we allow some second-neighbor jumps. We also find that the half-width is a very sensitive test for the existence of correlated jumps.

B. $v^{as}=\frac{1}{2}v^{ss}$

In this case the situation is quite different. The diffusion process is found to be more complicated and it is not possible to adjust α_2/α_1 in the jump model to get agreement with our calculated values, irrespectively of how the ratio α_2/α_1 is chosen. Our MCA result for the half-width is in Fig. 3(b) compared with the model with single uncorrelated jumps, and we notice a very large difference.

One can understand this through the following simple picture. We consider separately those adsorbed atoms that initially have energies below and above the energy barrier for diffusion. At the present temperature 78% of the atoms have the energies below the barrier and they need some energy from the lattice in order to escape from the initial cell. Since the friction is small in this case and hence also the fluctuating force, the particles will escape slowly. It is known⁸ that the absolute rate theory then

overestimates the escape rate. From $P_0(t)$ in Fig. 4(b) for $t^* > 2$ we get a number that is approximatively half of the ART value (12).

The remaining 22% of the atoms initially have energies above the energy barrier and they are able to escape quickly and to move several lattice distances before being stopped. The reason for this is again the small friction. They contribute very significantly to the total diffusion constant and this explains why our MCA value of $D^*=0.25$ is larger than the ART value of $D_{ART}^*=0.094$, despite the lower value of the escape rate above. Considering this smaller escape rate the effective jump distance, averaged over all adatoms, is about 2.1 lattice distances. These rapidly diffusing particles are not evident in the quasielastic peak in $S^s(q\omega)$, and the relatively small peak width in Fig. 3(b) reflects the motion of the more slowly diffusing atoms. However, they explain some of the features in the curves in Fig. 4(b). The cusp in the curve $P_0(t)$ around $t^*=1.5$ reflects the time when these rapidly moving particles have left the initial cell. The distribution in cells far away is then built up comparatively fast. Considering the time corresponding to $P_0(t)=0.30$, we have the following probabilities for the different cells shown in Fig. 4(b): 0.30, 0.16, 0.082, 0.045, 0.024, and 0.010. This should be compared with the other case, $v^{as}=v^{ss}$, where the corresponding values are 0.30, 0.20, 0.087, 0.029, 0.0074, and 0.0018.

VII. CONCLUSIONS

In this paper we have discussed the diffusive motion of an atom adsorbed on a solid surface. The investigation is based on a general microscopic theory for these processes¹ which can be applied equally well to diffusion in solids.⁹ The theory incorporates the dynamics of the adatom-substrate interaction in a more proper way than by using the Brownian motion theory. Deviations from the absolute rate theory (ART) for the escape rate and the mean jump distance can be determined.

The character of the diffusion process is quite clearly revealed through the q dependence in the width of the quasielastic peak in $S^s(q\omega)$. Due to the periodic mean density of the adatom, the width goes to zero at each reciprocal-lattice point. This happens for any temperature, provided the substrate surface forms a strictly periodic lattice structure. It is very different from what is found for a particle diffusing on a disordered surface, or when interaction with other adsorbed atoms becomes important.¹⁰ The q dependence in the width is very sensitive to the existence of correlated jumps, and by comparing the value at $q=\pi/a$ with the curvature at small q values one can get information on these aspects.

Two different cases have been considered, differing only with respect to the strength of the interaction between the adatom and a substrate atom. In the first case it was equal to the substrate-substrate atom interaction while in the second case it was reduced by a factor of 2. Both cases correspond essentially to activated diffusion with the activation energy being equal to $\Delta E=3.76k_B T$

and $\Delta E = 1.88k_B T$, respectively.

In the first case the diffusion process is very well described by a jump diffusion model with a small probability of second-neighbor jumps. The diffusion process is more complicated in the second case and this is due to the small value of the friction. Particles with initial energies above the potential barrier can move several lattice distances before being stopped and give a large contribution to the diffusion constant. On the other hand, particles having energy less than the barrier energy escape only slowly from their potential wells and give rise to a fairly sharp

quasielastic peak in $S^s(q\omega)$. These two aspects may be important when discussing the rate of different dynamical processes occurring at solid surfaces.

ACKNOWLEDGMENTS

The author would like to thank Professor A. Sjölander for many helpful discussions and for a very thorough and critical reading of the manuscript. Financial support from the Swedish Natural Science Research Council is also gratefully acknowledged.

¹G. Wahnström, *Surf. Sci.* **159**, 311 (1985), referred to as I.

²J. P. Boon and S. Yip, *Molecular Hydrodynamics* (McGraw-Hill, New York, 1980); T. Keyes, in *Statistical Mechanics, Part B: Time-Dependent Processes*, edited by B. J. Berne (Plenum, New York, 1977).

³G. Wahnström, *Surf. Sci.* (to be published), referred to as II.

⁴G. Ehrlich, *Surf. Sci.* **63**, 422 (1977).

⁵G. Ehrlich and K. Stolt, *Ann. Rev. Phys. Chem.* **31**, 603 (1980).

⁶S. Glasstone, K. J. Laidler, and H. Eyring, *The Theory of Rate*

Processes (McGraw-Hill, New York, 1941); G. Iche and Ph. Nozières, *J. Phys. (Paris)* **37**, 1313 (1976).

⁷This value for α^{ART} was used in I.

⁸H. A. Kramers, *Physica (Utrecht)* **7**, 284 (1940).

⁹W. G. Kleppmann and R. Zeyher, *Phys. Rev. B* **22**, 6044 (1980).

¹⁰H. Zabel, A. Magerl, A. J. Dianoux, and J. J. Rush, *Phys. Rev. Lett.* **50**, 2094 (1983); D. K. Chaturvedi and M. P. Tosi, *Z. Phys. B* **58**, 49 (1984).